hp-DGFEM for Maxwell's equations

Paul Houston[1,⋆], Ilaria Perugia[2], and Dominik Schötzau[3,⋆⋆]

[1] Department of Mathematics & Computer Science, University of Leicester, Leicester LE1 7RH, UK, email: Paul.Houston@mcs.le.ac.uk
[2] Dipartimento di Matematica, Università di Pavia, 27100 Pavia, Italy, email: perugia@dimat.unipv.it
[3] School of Mathematics, University of Minnesota, Minneapolis MN 55455, USA, email: schoetza@math.umn.edu

Abstract. We propose *hp*-version interior penalty discontinuous Galerkin methods for the discretization of the curl-curl operator with divergence free constraint, often encountered in electromagnetic problems. For unstructured meshes with hanging nodes, we present error estimates that are optimal in the meshsize h and slightly suboptimal in the polynomial approximation order p. The performance of these methods is numerically tested for two-dimensional model problems.

1 Introduction and Model Problem

Over the last few years there has been a renewed interest in discontinuous Galerkin finite element methods (DGFEM) applied to elliptic problems, see, e.g., [3] and the references therein. One of the reasons is that these methods easily handle discretizations with non-matching grids and variable approximation orders, and thus are ideally suited for *hp*-adaptivity and domain-decomposition approaches. The same reasons motivated the introduction of DGFEM for the time-harmonic Maxwell equations: in [8], an *hp*-adaptive local discontinuous Galerkin (LDG) method has been studied for the low-frequency approximation of these equations, and, in [9], an h-version interior penalty (IP) method has been used for discretizing the high-frequency time-harmonic Maxwell's equations in mixed form.

In this paper, we propose *hp*-version IP-DGFEM for the discretization of the curl-curl operator with divergence free constraint, often encountered in electromagnetic applications, such as the low-frequency time-harmonic Maxwell's problem in insulating materials or the magnetostatic problem in vector potential formulation with Coulomb gauge. The divergence free constraint is accounted for by a regularization approach as in [1], and the proposed methods involve IP discretizations of the curl-curl and grad-div operators. The *hp*-error analysis of these methods is carried out by adapting the unified setting for DGFEMs introduced in [2] for the h-version, as done in [8,7]

⋆ Paul Houston acknowledges the financial support of the EPSRC (GR/N24230).
⋆⋆ Supported in part by the National Science Foundation (Grant DMS-0107609) and by the University of Minnesota Supercomputing Institute.

for the *hp*-version of the LDG method. For unstructured meshes with hanging nodes, we recover the estimates of [6] (obtained with different techniques), which are optimal in h and slightly suboptimal in p. Numerical experiments demonstrating the performance of the IP-DGFEMs complete the paper.

The model problem we consider is the following:

$$\begin{aligned} \mathbf{curl}\,\mathbf{curl}\,\mathbf{u} &= \mathbf{f} \qquad \text{in } \Omega, \\ \operatorname{div}\mathbf{u} &= 0 \qquad \text{in } \Omega, \\ \mathbf{n}\times\mathbf{u} &= \mathbf{g} \qquad \text{on } \Gamma. \end{aligned} \tag{1}$$

Here, Ω is a bounded Lipschitz polyhedron in $\mathbb{R}^3$, with $\mathbf{n}$ denoting the outward normal unit vector to its boundary $\Gamma = \partial\Omega$. The datum $\mathbf{f}$ is an external source field satisfying $\operatorname{div}\mathbf{f} = 0$ in Ω and $\mathbf{f}\cdot\mathbf{n} = 0$ on Γ, and the Dirichlet datum $\mathbf{g}$ is a prescribed tangential trace which we assume to belong to $L^2(\Gamma)^3$. For simplicity, we assume here that Ω is simply-connected and that Γ is connected. The coefficients expressing the electromagnetic material properties have been taken equal to one; see [8] for extensions to more general cases.

We introduce the spaces $H(\mathrm{div};\Omega) = \{\mathbf{v}\in L^2(\Omega)^3 : \operatorname{div}\mathbf{v}\in L^2(\Omega)\}$ and $H(\mathbf{curl};\Omega) = \{\mathbf{v}\in L^2(\Omega)^3 : \mathbf{curl}\,\mathbf{v}\in L^2(\Omega)^3\}$, together with the subspace $H_0(\mathbf{curl};\Omega) = \{\mathbf{v}\in H(\mathbf{curl};\Omega) : \mathbf{n}\times\mathbf{v} = \mathbf{0}\}$, endowed with the graph norms, and the space $\mathbf{V} = \{\mathbf{v}\in H(\mathbf{curl};\Omega)\cap H(\mathrm{div};\Omega) : \mathbf{n}\times\mathbf{v}\in L^2(\Gamma)^3\}$, within which the analytical solution $\mathbf{u}$ to (1) belongs.

2 Discontinuous Galerkin Discretization

Here, we introduce IP-DGFEM for the discretization of (1), based on the following variational formulation: find $\mathbf{u}\in\mathbf{V}$ such that $\mathbf{n}\times\mathbf{u} = \mathbf{g}$ on Γ and

$$\int_\Omega \mathbf{curl}\,\mathbf{u}\cdot\mathbf{curl}\,\mathbf{v}\,d\mathbf{x} + \int_\Omega \operatorname{div}\mathbf{u}\,\operatorname{div}\mathbf{v}\,d\mathbf{x} = \int_\Omega \mathbf{f}\cdot\mathbf{v}\,d\mathbf{x} \tag{2}$$

for all $\mathbf{v}\in H_0(\mathbf{curl};\Omega)\cap H(\mathrm{div};\Omega)$. For any $\mathbf{f}\in L^2(\Omega)^3$, problem (2) has a unique solution $\mathbf{u}\in\mathbf{V}$ with $\mathbf{curl}\,\mathbf{u}\in H(\mathbf{curl};\Omega)$ and $\operatorname{div}\mathbf{u}\in H^1_0(\Omega)$. Moreover, the solution of (2) is also the solution to (1), provided that $\operatorname{div}\mathbf{f} = 0$ in Ω and $\mathbf{f}\cdot\mathbf{n} = 0$ on Γ.

2.1 Meshes, Finite Element Spaces and Traces

We consider shape regular meshes $\mathcal{T}_h$ that partition the domain Ω into tetrahedra and/or parallelepipeds, with possible hanging nodes. We denote by h_K the diameter of the element $K\in\mathcal{T}_h$ and set $h = \max_K h_K$. An *interior face* of $\mathcal{T}_h$ is defined as the (non-empty) two-dimensional interior of $\partial K^+\cap\partial K^-$, where K^+ and K^- are two adjacent elements of $\mathcal{T}_h$, not necessarily matching. A *boundary face* of $\mathcal{T}_h$ is defined as the (non-empty) two-dimensional interior of $\partial K \cap \Gamma$, where K is a boundary element of $\mathcal{T}_h$. We write $\mathcal{E}_\mathcal{I}$ to denote the union of all interior faces of $\mathcal{T}_h$, $\mathcal{E}_\mathcal{D}$ the union of all boundary faces of $\mathcal{T}_h$, and set $\mathcal{E} = \mathcal{E}_\mathcal{I} \cup \mathcal{E}_\mathcal{D}$. Moreover, we assign to each element $K \in \mathcal{T}_h$ a polynomial approximation order $p_K \geq 1$ and define the vector $\underline{p} = \{p_K\}_{K \in \mathcal{T}_h}$.

The generic finite element space of piecewise polynomials is given by

$$S^{\underline{p},0}(\mathcal{T}_h) := \{u \in L^2(\Omega) : u|_K \in \mathcal{S}^{p_K}(K) \quad \forall K \in \mathcal{T}_h\},$$

where $\mathcal{S}^{p_K}(K)$ is the space $\mathcal{P}^{p_K}(K)$ of polynomials of degree at most p_K in K, if K is a tetrahedron, and the space $\mathcal{Q}^{p_K}(K)$ of polynomials of degree at most p_K in each variable in K, if K is a parallelepiped.

For piecewise smooth vector- and scalar-valued functions $\mathbf{v}$ and φ, we introduce the following trace operators. Let $e \subset \mathcal{E}_\mathcal{I}$ be an interior face shared by two elements K^+ and K^-, and write $\mathbf{n}^\pm$ for the outward normal unit vectors to the boundaries $\partial K^\pm$, respectively. Denoting by $\mathbf{v}^\pm$ and $\varphi^\pm$ the traces on $\partial K^\pm$ taken from $K^\pm$, respectively, we define the *jumps* across e by

$$[\![\mathbf{v}]\!]_T = \mathbf{n}^+ \times \mathbf{v}^+ + \mathbf{n}^- \times \mathbf{v}^-, \quad [\![\mathbf{v}]\!]_N = \mathbf{v}^+ \cdot \mathbf{n}^+ + \mathbf{v}^- \cdot \mathbf{n}^-, \quad [\![\varphi]\!] = \varphi^+ \mathbf{n}^+ + \varphi^- \mathbf{n}^-,$$

and the *averages* $\{\!\{\mathbf{v}\}\!\} = (\mathbf{v}^+ + \mathbf{v}^-)/2$ and $\{\!\{\varphi\}\!\} = (\varphi^+ + \varphi^-)/2$. On a boundary face $e \subset \mathcal{E}_\mathcal{D}$, we set $[\![\mathbf{v}]\!]_T = \mathbf{n} \times \mathbf{v}$, $[\![\varphi]\!] = \varphi \mathbf{n}$, $\{\!\{\mathbf{v}\}\!\} = \mathbf{v}$ and $\{\!\{\varphi\}\!\} = \varphi$.

2.2 Interior Penalty Method

Let $\mathbf{V}_h = S^{\underline{p},0}(\mathcal{T}_h)^3$. The IP-DGFEM is defined by: find $\mathbf{u}_h \in \mathbf{V}_h$ such that

$$\mathcal{A}_h(\mathbf{u}_h, \mathbf{v}) + \mathcal{I}_h(\mathbf{u}_h, \mathbf{v}) = \mathcal{F}_h(\mathbf{v}) \tag{3}$$

for all $\mathbf{v} \in \mathbf{V}_h$, where

$$\begin{aligned}
\mathcal{A}_h(\mathbf{u}, \mathbf{v}) = & \int_\Omega \mathbf{curl}_h\, \mathbf{u} \cdot \mathbf{curl}_h\, \mathbf{v} \, d\mathbf{x} - \int_\mathcal{E} [\![\mathbf{u}]\!]_T \cdot \{\!\{\mathbf{curl}_h\, \mathbf{v}\}\!\} \, ds \\
& - \int_\mathcal{E} [\![\mathbf{v}]\!]_T \cdot \{\!\{\mathbf{curl}_h\, \mathbf{u}\}\!\} \, ds + \int_\Omega \operatorname{div}_h \mathbf{u} \, \operatorname{div}_h \mathbf{v} \, d\mathbf{x} \\
& - \int_{\mathcal{E}_\mathcal{I}} [\![\mathbf{u}]\!]_N \, \{\!\{ \operatorname{div}_h \mathbf{v}\}\!\} \, ds - \int_{\mathcal{E}_\mathcal{I}} [\![\mathbf{v}]\!]_N \, \{\!\{ \operatorname{div}_h \mathbf{u}\}\!\} \, ds, \\
\mathcal{I}_h(\mathbf{u}, \mathbf{v}) = & \int_\mathcal{E} \mathtt{a} \, [\![\mathbf{u}]\!]_T \cdot [\![\mathbf{v}]\!]_T \, ds + \int_{\mathcal{E}_\mathcal{I}} \mathtt{b} \, [\![\mathbf{u}]\!]_N \, [\![\mathbf{v}]\!]_N \, ds, \\
\mathcal{F}_h(\mathbf{v}) = & \int_\Omega \mathbf{f} \cdot \mathbf{v} \, d\mathbf{x} - \int_{\mathcal{E}_\mathcal{D}} \mathbf{g} \cdot \mathbf{curl}_h\, \mathbf{v} \, ds + \int_{\mathcal{E}_\mathcal{D}} \mathtt{a} \, \mathbf{g} \cdot (\mathbf{n} \times \mathbf{v}) \, ds.
\end{aligned}$$

Here, $\mathbf{curl}_h$ and div_h are the elementwise curl and divergence operators, respectively. The parameters $\mathtt{a}, \mathtt{b} \in L^\infty(\mathcal{E})$ are the discontinuity stabilization parameters; these are chosen in terms of the local meshsize and approximation degree as follows. Define $\mathtt{h}$ and $\mathtt{p}$ in $L^\infty(\mathcal{E})$ by $\mathtt{h}(\mathbf{x}) = \min\{h_K, h_{K'}\}$ and

$\mathtt{p}(\mathbf{x}) = \max\{p_K, p_{K'}\}$, if $\mathbf{x}$ is in the interior of $\partial K \cap \partial K'$, and by $\mathtt{h}(\mathbf{x}) = h_K$ and $\mathtt{p}(\mathbf{x}) = p_K$, if $\mathbf{x}$ is in the interior of $\partial K \cap \Gamma$. Then we set

$$\mathtt{a} = \alpha \, \frac{\mathtt{p}^2}{\mathtt{h}}, \qquad \mathtt{b} = \beta \, \frac{\mathtt{p}^2}{\mathtt{h}},$$

with parameters α and β independent of $\mathtt{h}$ and $\mathtt{p}$, but large enough to guarantee the stability of the method (see Proposition 1 below).

Using the same arguments as in [9, Proposition 4] and [8, Theorem 3.3], it is easy to see that the IP-DGFEM is consistent, i.e., the exact solution $\mathbf{u}$ of problem (1) satisfies (3), for all test functions $\mathbf{v} \in \mathbf{V}_h$.

Remark 1. The non-symmetric variant of the interior penalty method (NIP) is obtained by changing the sign in front of the second and fifth terms in the form $\mathcal{A}_h$, and in front of the second term on the right-hand side of $\mathcal{F}_h$.

3 Error Analysis

In this section, we develop the *hp*-error analysis for our methods, following the work presented in [8].

First, we rewrite the IP-DGFEM in terms of lifting operators as in [2] and [8]. To this end, we introduce the auxiliary space $Q_h := S^{\underline{p},0}(\mathcal{T}_h)$, and define the operators $\mathcal{L} : L^2(\mathcal{E})^3 \to \mathbf{V}_h$ and $\mathcal{M} : L^2(\mathcal{E}_\mathcal{I}) \to Q_h$ by

$$\int_\Omega \mathcal{L}(\mathbf{v}) \cdot \mathbf{w} \, d\mathbf{x} = \int_\mathcal{E} \mathbf{v} \cdot \{\!\{\mathbf{w}\}\!\} \, ds, \qquad \int_\Omega \mathcal{M}(v) \, p \, d\mathbf{x} = \int_{\mathcal{E}_\mathcal{I}} v \, \{\!\{p\}\!\} \, ds$$

for all $\mathbf{w} \in \mathbf{V}_h,\ p \in Q_h$, respectively.

Then, we introduce the discontinuous Galerkin form $\mathcal{A}_h^{\mathrm{lift}}$ given by

$$\begin{aligned}
\mathcal{A}_h^{\mathrm{lift}}(\mathbf{u}, \mathbf{v}) = & \int_\Omega \mathbf{curl}_h \, \mathbf{u} \cdot \mathbf{curl}_h \, \mathbf{v} \, d\mathbf{x} - \int_\Omega \mathcal{L}([\![\mathbf{u}]\!]_T) \cdot \mathbf{curl}_h \, \mathbf{v} \, d\mathbf{x} \\
& - \int_\Omega \mathcal{L}([\![\mathbf{v}]\!]_T) \cdot \mathbf{curl}_h \, \mathbf{u} \, d\mathbf{x} + \int_\Omega \operatorname{div}_h \mathbf{u} \, \operatorname{div}_h \mathbf{v} \, d\mathbf{x} \\
& - \int_\Omega \mathcal{M}([\![\mathbf{u}]\!]_N) \, \operatorname{div}_h \mathbf{v} \, d\mathbf{x} - \int_\Omega \mathcal{M}([\![\mathbf{v}]\!]_N) \, \operatorname{div}_h \mathbf{u} \, d\mathbf{x}.
\end{aligned}$$

Notice that the forms $\mathcal{A}_h$ and $\mathcal{A}_h^{\mathrm{lift}}$ coincide whenever both arguments belong to $\mathbf{V}_h$. This is no longer true for functions in $\mathbf{V}$, due to the polynomial nature of the liftings. On the other hand, the form $\mathcal{B}_h(\mathbf{u}, \mathbf{v}) := \mathcal{A}_h^{\mathrm{lift}}(\mathbf{u}, \mathbf{v}) + \mathcal{I}_h(\mathbf{u}, \mathbf{v})$ has the continuity and coercivity properties that allow us to carry out the analysis of our methods in a straightforward way by Strang's lemma, as already done in [7,8] for the LDG method.

We set $\mathbf{V}(h) = \mathbf{V}_h + \mathbf{V}$, endowed with the DG-norm

$$|\!|\!|\mathbf{v}|\!|\!|_h^2 = \| \mathbf{curl}_h \, \mathbf{v}\|_{0,\Omega}^2 + \| \operatorname{div}_h \mathbf{v}\|_{0,\Omega}^2 + \|\mathtt{h}^{-\frac{1}{2}} \mathtt{p} \, [\![\mathbf{v}]\!]_T\|_{0,\mathcal{E}}^2 + \|\mathtt{h}^{-\frac{1}{2}} \mathtt{p} \, [\![\mathbf{v}]\!]_N\|_{0,\mathcal{E}_\mathcal{I}}^2.$$

The following continuity and stability results hold true.

Proposition 1. *Under the above assumptions we have that*

$$|\mathcal{B}_h(\mathbf{w},\mathbf{v})| \leq C_{\mathrm{cont}} |||\mathbf{w}|||_h |||\mathbf{v}|||_h \qquad \forall \mathbf{w},\mathbf{v} \in \mathbf{V}(h),$$

for any $\alpha, \beta > 0$. Moreover,

$$\mathcal{B}_h(\mathbf{v},\mathbf{v}) \geq C_{\mathrm{coer}} |||\mathbf{v}|||_h^2 \qquad \forall \mathbf{v} \in \mathbf{V}_h,$$

provided that $\alpha \geq \alpha_{\max}$, $\beta \geq \beta_{\max}$, with $\alpha_{\max}$ and $\beta_{\max}$ solely depending on the shape-regularity of the mesh. The constants C_{cont} and C_{coer} only depend on α, β and the shape-regularity of the mesh.

Proof. We note that from [8, Proposition 4.2] there exists a constant C_{lift} depending only on the shape-regularity of the mesh such that $\|\mathcal{L}([\![\mathbf{v}]\!]_T)\|_{0,\Omega} \leq C_{\mathrm{lift}} \|\mathbf{h}^{-\frac{1}{2}}\mathbf{p}\, [\![\mathbf{v}]\!]_T\|_{0,\mathcal{E}}$ and $\|\mathcal{M}([\![\mathbf{v}]\!]_N)\|_{0,\Omega} \leq C_{\mathrm{lift}} \|\mathbf{h}^{-\frac{1}{2}}\mathbf{p}\, [\![\mathbf{v}]\!]_N\|_{0,\mathcal{E}_{\mathcal{I}}}$, for all $\mathbf{v} \in \mathbf{V}(h)$. The above continuity and coercivity properties can be obtained from these estimates as in [2], by the Cauchy-Schwarz inequality and the geometric-arithmetic mean inequality $ab \leq \delta^{-1}a^2 + \delta b^2$ for all $\delta > 0$.

From now on, we assume that α and β are large enough to ensure that the stability result of Proposition 1 holds. By employing Strang's lemma, we obtain the following abstract error bound.

Theorem 1. *Under the above assumptions we have*

$$|||\mathbf{u}-\mathbf{u}_h|||_h \leq \left(1+\frac{C_{\mathrm{cont}}}{C_{\mathrm{coer}}}\right) \inf_{\mathbf{v}\in\mathbf{V}_h} |||\mathbf{u}-\mathbf{v}|||_h + \frac{1}{C_{\mathrm{coer}}} R_h(\mathbf{u}),$$

where $R_h(\mathbf{u})$ is given by $R_h(\mathbf{u}) = \sup_{\mathbf{0}\neq\mathbf{w}\in\mathbf{V}_h} \dfrac{|\mathcal{B}_h(\mathbf{u},\mathbf{w}) - \mathcal{F}_h(\mathbf{w})|}{|||\mathbf{w}|||_h}$.

We start by estimating $R_h(\mathbf{u})$; to this end, we have the following result.

Proposition 2. *Assume $\mathbf{u}|_K \in H^{s_K+1}(K)^3$ for all $K \in \mathcal{T}_h$ and $s_K \geq 1$. Then,*

$$R_h(\mathbf{u})^2 \leq C \sum_{K\in\mathcal{T}_h} \frac{h_K^{2\min(p_K+1,s_K)}}{p_K^{2s_K}} \|\mathbf{u}\|_{s_K+1,K}^2.$$

Proof. It can be easily seen that under the above smoothness assumptions,

$$\begin{aligned} \mathcal{B}_h(\mathbf{u},\mathbf{v}) - \mathcal{F}_h(\mathbf{v}) = &\int_{\mathcal{E}} [\![\mathbf{v}]\!]_T \cdot \{\!\{\mathbf{curl}_h\,\mathbf{u} - \Pi_{\mathbf{V}_h}(\mathbf{curl}_h\,\mathbf{u})\}\!\}\, ds \\ &+ \int_{\mathcal{E}_{\mathcal{I}}} [\![\mathbf{v}]\!]_N \{\!\{\mathrm{div}_h\,\mathbf{u} - \Pi_{Q_h}(\mathrm{div}_h\,\mathbf{u})\}\!\}\, ds, \end{aligned} \tag{4}$$

with $\Pi_{\mathbf{V}_h}$ and Π_{Q_h} denoting the L^2-projections onto $\mathbf{V}_h$ and Q_h, respectively. The estimate of the residual follows as in [8].

Remark 2. From Theorem 1 and (4), we see that, for solutions $\mathbf{u}$ that are analytic in $\overline{\Omega}$, the p-version DG method gives exponential convergence rates.

Next, hp-error estimates on general unstructured meshes with hanging nodes can be derived as in [8], under the assumption that there exists a constant $\ell > 0$ such that $\ell^{-1} h_K \leq h_{K'} \leq \ell h_K$ and $\ell^{-1} p_K \leq p_{K'} \leq \ell p_K$ for all K and K' sharing a two-dimensional face.

Theorem 2. *Assume the above hypotheses on the numerical fluxes, meshes and polynomial degree distributions hold. Let the exact solution* $\mathbf{u}$ *satisfy* $\mathbf{u}|_K \in H^{s_K+1}(K)^3$, *with local regularity exponents* $s_K \geq 1$. *Then,*

$$\|\!|\mathbf{u} - \mathbf{u}_h\|\!|_h^2 \leq C \sum_{K \in \mathcal{T}_h} \frac{h_K^{2\min(p_K, s_K)}}{p_K^{2s_K - 1}} \|\mathbf{u}\|_{s_K+1,K}^2,$$

with a constant C *independent of* h_K *and* p_K.

Remark 3. The bounds in Theorem 2 are slightly suboptimal in the orders p_K. On affine quadrilateral meshes in two dimensions with hanging nodes, the p-bounds can be improved by using the projector of [5], provided that $\mathbf{u}$ belongs to an augmented Sobolev space.

4 Numerical results

In this section, we present a series of numerical experiments to verify the *a priori* error estimates derived in Section 3. Here, we set $\alpha = \beta = 10$ and restrict ourselves to two-dimensional model problems only. In this case the "curl" operators have to be understood as follows. If $\mathbf{v} = (v_1, v_2)$ is a vector field, then $\operatorname{curl} \mathbf{v}$ is the scalar field $\operatorname{curl} \mathbf{v} = \frac{\partial v_2}{\partial x} - \frac{\partial v_1}{\partial y}$, whereas if φ is a scalar field, then $\mathbf{curl}\,\varphi$ is the vector field $\mathbf{curl}\,\varphi = \left(\frac{\partial \varphi}{\partial y}, -\frac{\partial \varphi}{\partial x}\right)$. On the boundary, we have $\mathbf{n} \times \mathbf{u} = \mathbf{u} \cdot \mathbf{t}$, where $\mathbf{t}$ is the counterclockwise oriented tangential unit vector. Hence, the Dirichlet boundary datum is a scalar function g. Similarly, the tangential jumps are scalar quantities defined as $[\![\mathbf{v}]\!]_T = \mathbf{v}^+ \cdot \mathbf{t}^+ + \mathbf{v}^- \cdot \mathbf{t}^-$.

Example 1. Here, we let Ω be the L-shaped domain shown in Figure 1; further, we choose $\mathbf{f}$ so that the analytical solution to (1) is given by

$$\mathbf{u}(x, y) = \begin{pmatrix} -\exp(x)(y\cos(y) + \sin(y)) \\ \exp(x) y \sin(y) \end{pmatrix}. \tag{5}$$

We investigate the asymptotic behavior of the hp-version of the IP-DGFEM on a sequence of successively finer square and quadrilateral meshes for different p. In each case the quadrilateral mesh is constructed from a uniform square mesh by randomly perturbing each of the *interior* nodes by up to 10% of the local mesh-size, cf. [6].

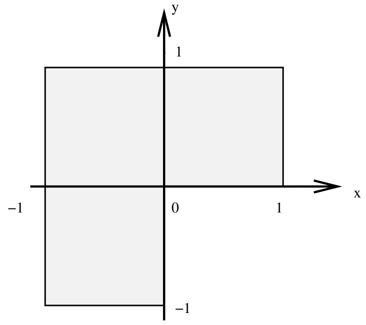

Fig. 1. L-shaped domain Ω.

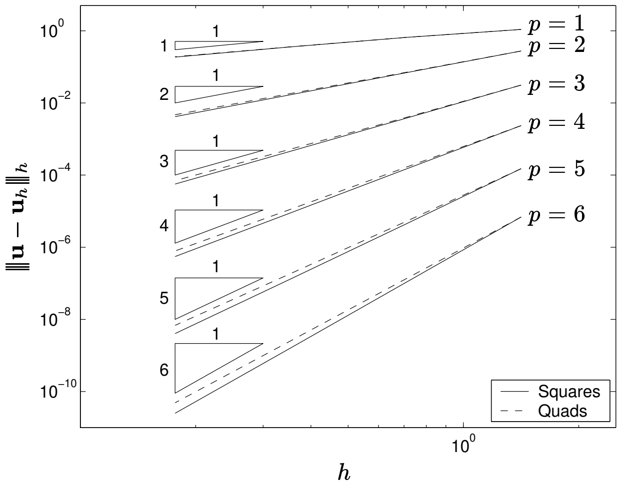

Fig. 2. Example 1. Convergence of the IP-DGFEM with h-refinement.

In Figure 2 we present a comparison of the DG-norm $\|\cdot\|_h$ of the error with the mesh function h for $1 \leq p \leq 6$. Here, we observe that $\|\mathbf{u}-\mathbf{u}_h\|_h$ converges to zero, for each fixed p, at the rate $\mathcal{O}(h^p)$ as the mesh is refined, thereby confirming Theorem 2. Secondly, we investigate the convergence of the IP-DGFEM with p-enrichment on a fixed mesh. Since the true solution (5) is a real analytic function, we expect to see exponential rates of convergence as p increases. In Figure 3, we plot the DG-norm of the error against p on four different square and quadrilateral meshes. In each case, we observe that on a linear-log scale, the convergence plots become straight lines as the spectral order p is increased, thereby indicating exponential convergence in p, cf. Remark 2. Furthermore, we observe from Figures 2 and 3 that the h- and p-convergence of the IP-DGFEM is robust with respect to mesh distortion.

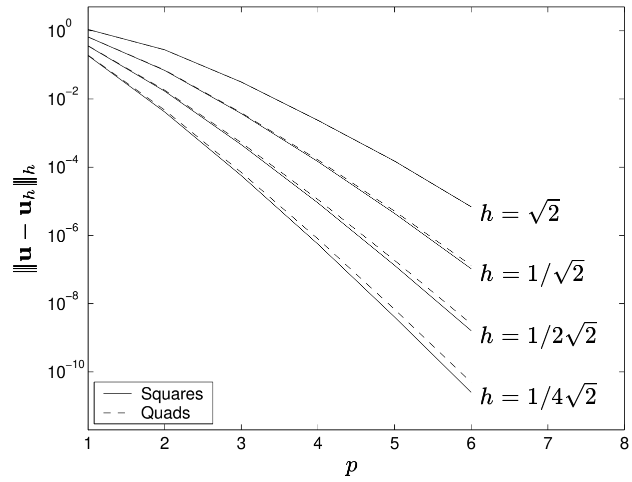

Fig. 3. Example 1. Convergence of the IP-DGFEM with p-refinement.

Finally, we note that the asymptotic behavior of (unsymmetric) NIP-DGFEM is analogous to the (symmetric) IP-DGFEM presented above. By this we mean that the DG-norm of the error converges to zero, for each fixed p, at the rate $\mathcal{O}(h^p)$ as the mesh is refined, and exponential rates of convergence are observed as p is increased for fixed h. We remark that the key difference in the numerical performance of the symmetric and unsymmetric versions of the hp-DGFEM is observed when the error is measured in terms of the $L^2(\Omega)$ norm, rather than the DG-norm. In this case, the error in the IP-DGFEM decays to zero at the optimal rate $\mathcal{O}(h^{p+1})$ for fixed p as h tends to zero. In contrast, the latter (unsymmetric) scheme is only optimal for odd p; more precisely, we observe that the error in the $L^2(\Omega)$-norm behaves like $\mathcal{O}(h^{p+1})$ for odd p and like $\mathcal{O}(h^p)$ for even p, cf. [6].

Example 2. In this second example, we investigate the performance of the IP-DGFEM and the NIP-DGFEM for a problem in which the precise regularity of the analytical solution $\mathbf{u}$ is known. To this end, we again let Ω be the L-shaped domain shown in Figure 1; here, we set $\mathbf{f} = \mathbf{0}$ and $\mathbf{g}$ is chosen so that the analytical solution to (1) is given, in terms of the polar coordinates (r, ϑ), by

$$\mathbf{u}(x,y) = \nabla S(r,\vartheta), \quad \text{where} \quad S(r,\vartheta) = r^{2n/3}\sin(2n\vartheta/3) \tag{6}$$

and $n > 1$ is a parameter. The analytical solution given by (6) contains a singularity at the corner located at the origin of Ω; here, $\mathbf{u} \in H^{2n/3}(\Omega)^2$.

In Figure 4 we present a comparison of the DG-norm of the error with the mesh function h, on uniform square meshes for $1 \le p \le 6$ and $n = 8$. Here, we observe that for both the IP-DGFEM and the NIP-DGFEM the error

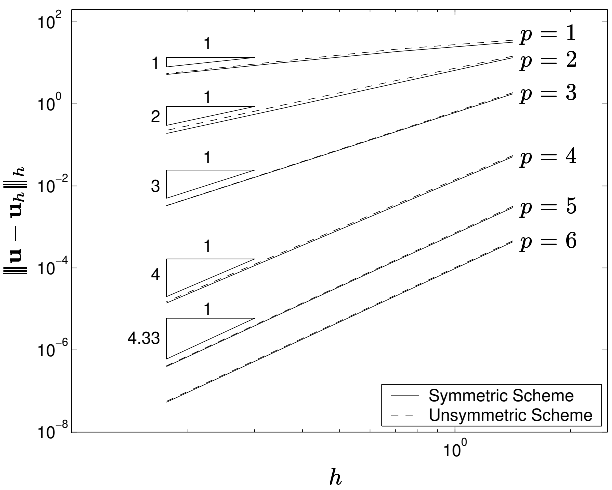

Fig. 4. Example 2. Convergence of the IP- and NIP-DGFEM with h-refinement.

$\|\mathbf{u} - \mathbf{u}_h\|_h$ converges to zero at the optimal rate $\mathcal{O}(h^{\min(p,2n/3-1)})$, $n = 8$, cf. Theorem 2. We remark that the same behavior is also observed on both quasi-uniform quadrilateral meshes and for different values of n; for brevity, these results have been omitted.

Finally, we investigate the asymptotic behavior of the proposed methods with p enrichment. In Table 1 we show the the DG-norm of the error and the computed rate of convergence k for the IP-DGFEM for $n = 8$, 4 and 2, on a uniform square mesh consisting of three elements. Here, we observe that the DG-norm of the error converges to zero at (approximately) the rate $\mathcal{O}(p^{-2(2n/3-1)})$; this is twice the (optimal) rate predicted by Theorem 2. However, this behavior is due to the presence of the singularity in $\mathbf{u}$ arising on an inter-element boundary, rather than in the interior of an element K in the mesh. Indeed, by employing approximation results in terms of weighted Sobolev norms, *a priori* error bounds which reflect this order doubling in the rate of convergence of the IP-DGFEM with p refinement may be established, cf. [6]. Similar behavior is observed with the NIP-DGFEM.

5 Conclusions

We proposed discontinuous Galerkin methods for the Maxwell operator that are based on interior penalty techniques to enforce the continuity of the electromagnetic fields. An hp-error analysis has been carried out under the assumption of piecewise smooth regular solutions. For singular solutions with $n = 1$, numerical experiments not reported here have shown that the joint use of these methods and the weighted regularization technique of [4] give good results. Ad hoc variants for discontinuous methods are under investigation.

	$n=8$		$n=4$		$n=2$	
p	$\|\|\|\mathbf{u}-\mathbf{u}_h\|\|\|_h$	k	$\|\|\|\mathbf{u}-\mathbf{u}_h\|\|\|_h$	k	$\|\|\|\mathbf{u}-\mathbf{u}_h\|\|\|_h$	k
1	32.03	-	2.202	-	0.5662	-
2	13.37	1.26	0.1895	3.54	0.4998	0.18
3	1.760	5.00	5.121e-02	3.23	0.4275	0.39
4	5.130e-02	12.3	2.092e-02	3.11	0.3753	0.45
5	2.975e-03	12.8	1.050e-02	3.09	0.3362	0.49
6	4.322e-04	10.6	5.986e-03	3.08	0.3058	0.52
7	9.675e-05	9.71	3.718e-03	3.09	0.2814	0.54
8	2.806e-05	9.27	2.458e-03	3.10	0.2614	0.55
9	9.704e-06	9.02	1.704e-03	3.11	0.2446	0.57
10	3.817e-06	8.86	1.226e-03	3.12	0.2302	0.57
11	1.657e-06	8.75	9.097e-04	3.13	0.2178	0.58
12	7.788e-07	8.68	6.920e-04	3.14	0.2069	0.59
13	3.904e-07	8.63	5.377e-04	3.15	0.1973	0.59
14	2.065e-07	8.59	4.254e-04	3.16	0.1888	0.60
15	1.144e-07	8.57	3.419e-04	3.17	0.1811	0.60

Table 1. Example 2. Convergence of the IP-DGFEM with p-refinement.

References

1. A. Alonso and A. Valli. A domain decomposition approach for heterogeneous time-harmonic Maxwell equations. *Comput. Meth. Appl. Mech. Engrg.*, 143:97–112, 1997.
2. D.N. Arnold, F. Brezzi, B. Cockburn, and L.D. Marini. Unified analysis of discontinuous Galerkin methods for elliptic problems. *SIAM J. Numer. Anal.* (to appear).
3. B. Cockburn, G.E. Karniadakis, and C.-W. Shu, editors. *Discontinuous Galerkin Methods. Theory, Computation and Applications*, volume 11 of *Lect. Notes Comput. Sci. Eng.* Springer, 2000.
4. M. Dauge, M. Costabel, and D. Martin. Weighted regularization of Maxwell equations in polyhedral domains. Preprint, University of Rennes, 2001.
5. E.H. Georgoulis and E. Süli. *hp*-DGFEM on shape-irregular meshes: reaction-diffusion. Technical Report NA 01–09, Oxford University Computing Laboratory, 2001.
6. P. Houston, C. Schwab, and E. Süli. Discontinuous *hp*-finite element methods for advection-diffusion-reaction problems. *SIAM J. Numer. Anal.*, (to appear).
7. I. Perugia and D. Schötzau. An *hp*-analysis of the local discontinuous Galerkin method for diffusion problems. *J. Sci. Comput.* (to appear).
8. I. Perugia and D. Schötzau. The *hp*-local discontinuous Galerkin method for low-frequency time-harmonic Maxwell's equations. Technical Report 1774, IMA, University of Minnesota, 2001.
9. I. Perugia, D. Schötzau, and P. Monk. Stabilized interior penalty methods for the time-harmonic Maxwell equations. Technical Report 101, MSI, University of Minnesota, 2001.